Effects of Relative and Absolute Sea Surface Temperature on Tropical Cyclone Potential Intensity Using a Single-Column Model

HAMISH A. RAMSAY

NASA Goddard Institute for Space Studies, and Department of Applied Physics and Applied Mathematics, Columbia University, New York, New York

ADAM H. SOBEL

Department of Applied Physics and Applied Mathematics, and Department of Earth and Environmental Sciences, and Lamont-Doherty Earth Observatory, Columbia University, New York, New York

(Manuscript received 24 February 2010, in final form 1 July 2010)

ABSTRACT

The effects of relative and absolute sea surface temperature (SST) on tropical cyclone potential intensity are investigated using the Massachusetts Institute of Technology (MIT) single-column model. The model is run in two modes: (i) radiative–convective equilibrium (RCE) to represent the convective response to uniform warming of the ocean as in a homogeneous aqua planet, and (ii) weak temperature gradient (WTG) to represent the convective response to warming over a limited area of ocean while the SST outside that area remains unchanged. The WTG calculations are taken to represent the sensitivity of the atmospheric state to relative SST changes, while the RCE calculations are taken to represent the sensitivity to absolute SST changes occurring in the absence of relative SST changes. The potential intensity is computed using temperature and moisture profiles from the two sets of experiments for various values of SST. The computed potential intensity is more sensitive to relative SST than to absolute SST, with slopes of between about 7 and 8 m s^{-1} $°C^{-1}$ (depending on choice of input parameters in the model's convection scheme and other details of the model configuration) in the WTG calculations and about 1 m s^{-1} $°C^{-1}$ in RCE. The sensitivity to relative SST obtained from these calculations is quantitatively similar to that obtained previously by G. Vecchi and B. J. Soden from global climate model output. The greater sensitivity of potential intensity to SST in the WTG simulations (relative to RCE) can be attributed primarily to larger changes in the air–sea thermodynamic disequilibrium in those calculations as SST changes, which results from the inability of the free troposphere to adjust to the SST in WTG as it does in RCE.

1. Introduction

In recent years, much attention has been given to understanding the links between tropical cyclone (TC) intensity and those environmental factors that act as controls on TC intensity. Several studies have implicated increasing sea surface temperature (SST), at least partially forced by increased greenhouse gases, as a direct cause of a concomitant increase in TC intensity for some ocean basins (e.g., Webster et al. 2005; Hoyos et al. 2006), particularly for the North Atlantic basin (e.g., Emanuel 2005). The trends in TC activity found in these studies have been questioned because of changes over time in the observing system (e.g., Landsea et al. 2006), inspiring increased effort to resolve these issues (e.g., Kossin et al. 2007; Kruk et al. 2010).

Compared to the other basins, the TC intensity data are the most reliable in the North Atlantic as a result of routine aircraft measurements. Particularly since the early 1970s (when satellite data are also available) there has been a strong positive correlation between SST and integrated measures of TC activity such as the accumulated cyclone energy (ACE) and power dissipation index (PDI), with a near doubling of PDI over about 35 years. If this relationship were to continue into the future, based on climate model projections the North Atlantic PDI would increase at an alarming rate (Vecchi et al. 2008).

An alternative hypothesis is that changes in TC activity are controlled not by the absolute value of the SST,

Corresponding author address: Hamish A. Ramsay, NASA Goddard Institute for Space Studies, 2880 Broadway, New York, NY 10025.
E-mail: hramsay@giss.nasa.gov

DOI: 10.1175/2010JCLI3690.1

but its relative value (Vecchi and Soden 2007; Swanson 2008; Vecchi et al. 2008)—that is, the local SST relative to some measure of SST (such as its spatial mean) in the rest of the tropics. During the last few decades, the increase in Atlantic SST exceeded that in the tropical mean. Since relative and absolute SST both increased during this period, it is impossible to determine from the recent observational record which one is the more important reason for the observed TC trends. Yet determining which is more important has major implications for the future, since there is no reason to think that future warming in the Atlantic will continue to exceed that elsewhere.

Potential intensity (PI) (Emanuel 1986; Holland 1997; Bister and Emanuel 1998) is a measure of the theoretical maximum intensity a TC can attain given the local environmental values of certain thermodynamic variables, namely SST and tropospheric profiles of temperature and moisture. While PI theory has been challenged on theoretical grounds (Smith et al. 2008; Montgomery et al. 2009), the recent thorough assessment by Bryan and Rotunno (2009) in the context of an axisymmetric numerical model shows that given the constraints inherent to the framework of an axisymmetric theory that predicts maximum TC intensity based on the large-scale environment alone—constraints whose relaxation would inevitably lead to a much more complicated theory—it is difficult to improve upon it. PI theory has also passed some observational tests (e.g., Wing et al. 2007). PI remains a useful tool to study the relationship between TCs and their environment.

Vecchi and Soden (2007) showed that the relative SST is a good proxy for PI, using both global climate model (GCM) projections of future climate and historical reanalysis data. The physical argument supporting this is straightforward. Tropical upper-tropospheric temperature is approximately uniform in the horizontal, and its value is controlled by the tropical mean SST [or perhaps the mean over just those regions where deep convection is frequent (Sobel et al. 2002)], while the PI is sensitive to both the local SST and the local tropospheric temperature profile. A warming (cooling) of the surface, which is limited to a small fraction of the tropics, acts to warm and moisten (cool and dry) the atmospheric boundary layer locally, but does not cause changes of similar magnitude in the free-tropospheric temperature since the latter must remain approximately uniform horizontally. Such a warming (cooling) thus destabilizes (stabilizes) the overlying atmosphere, altering PI.

In the spirit of the hierarchical modeling approach (e.g., Held 2005), in this study we bridge the gap between estimates of PI sensitivity to relative and absolute SST based on observations and GCM simulations on the one hand, and qualitative theoretical arguments (as given above) used to interpret those estimates on the other. We use a single-column model that is one-dimensional, and thus much simpler than a GCM, yet still has explicit parameterizations of radiative and convective physics at the same level of complexity as those in GCMs. Large-scale dynamics is parameterized by the weak temperature gradient (WTG) approximation. Our approach is different than that used in other studies that have used idealized models to address the relationship of PI to SST (Schade 2000; Pasquero and Emanuel 2008). The emphasis of those studies was on ocean feedbacks, while ours focuses more on the role of the large-scale atmospheric response to given SST.

2. Single-column model experiments

We use the single-column model described in Bony and Emanuel (2001), based on the earlier model of Rennó et al. (1994 a,b). The convection scheme in the model is an updated and modified version of Emanuel (1991), as presented in Emanuel and Živković-Rothman (1999). The radiative parameterization schemes of Fouquart and Bonnel (1980) and Morcrette (1991) are used as well as an interactive cloud-radiative scheme developed by Bony and Emanuel (2001). Surface latent and sensible heat fluxes are parameterized by bulk aerodynamic formulas, including a gust factor that depends on convective downdrafts. The model is forced at the lower boundary by SST, surface albedo, and surface wind speed, all of which are fixed for each set of simulations. The surface albedo is set to 0.05. The surface wind speed is held constant at 7 m s^{-1} for all simulations except those in section 3c, which addresses the sensitivity of changes in PI to changes in surface wind speed. The CO_2 is fixed at 380 ppm and the insolation is set to 400 W m^{-2} with a zenith angle of zero degrees so that there is no diurnal cycle. The model time step is 5 min for the first set of experiments and 3 min for the second set (see details below). The smaller time step in the second set of experiments was necessary to avoid numerical instability for SST above 29°C.

We use 54 levels in the vertical, with 25-hPa grid spacing between the surfaces and 175 hPa and higher resolution above to more accurately resolve the tropopause. A uniform 25-hPa resolution throughout the troposphere resulted in some noisy behavior when calculating PI because the tropopause was poorly resolved and the PI was sensitive to the tropopause height.

To explore the sensitivity of PI to changes in absolute SST and relative SST we conduct two sets of experiments. The first set—referred to herein as the radiative–convective equilibrium (RCE) simulations—is designed to test the sensitivity of PI to changes in absolute SST

alone, as in an aqua planet with SST that is spatially uniform but differs from one climate state to the next. The second set tests the sensitivity of PI to changes in relative SST using the WTG approximation (e.g., Sobel and Bretherton 2000). This represents SST change over a limited area while the rest of the tropical SST remains unchanged.

In RCE mode, large-scale vertical velocity is assumed to vanish. In steady state, radiative cooling and convective heating must balance (up to sensible heat flux, which we assume to be small over tropical oceans), and surface evaporation must equal precipitation. The temperature profile tends to be approximately moist adiabatic from the surface to the tropopause, and nearly neutral to moist convection (but not quite neutral, so that convection persists).

In WTG mode, large-scale vertical velocity is parameterized rather than neglected in the thermodynamic equations. In the free troposphere, the temperature profile is specified to remain constant, consistent with the assumption that the temperature tendency is zero. This assumption allows the free-tropospheric vertical velocity to be diagnosed interactively, as that which is required to balance diabatic heating and adiabatic cooling. Horizontal temperature advection is neglected, a reasonable approximation in the tropics because horizontal temperature gradients are small there. The resulting vertical velocity is then used together with the prognostic moisture field to calculate the vertical moisture advection. The interactive computation of moisture advection renders the total vertically integrated moisture convergence also interactive, so that surface evaporation and precipitation need not be equal in steady state (as they must be in RCE). Within the boundary layer, the temperature is left as a prognostic variable and the vertical velocity is specified by linearly interpolating ω from its value at the boundary layer–free troposphere interface to zero at the surface.

As a crude representation of horizontal moisture advection, the tropospheric specific humidity profile is relaxed back to a reference profile (the steady-state RCE solution for SST = 27.5°C) with a relaxation time of three days. The relaxation time scale is the length scale of horizontal moisture gradients (~2000 km) over a typical horizontal wind velocity (~8 m s^{-1}). This representation of horizontal moisture advection is identical to that used by Sobel et al. (2007), and similar but not identical to that used in other recent studies using WTG in single-column or cloud-resolving models (e.g., Raymond and Zeng 2005; Sobel and Bellon 2009; Sessions et al. 2010). The sensitivity of our primary results to this modeling choice is small, as discussed further below.

For a specified SST, we first run the model for a sufficient amount of time in order to reach a state of RCE. A statistical equilibrium is generally reached after about 60 days of integration. We let the model run for 180 days in total and take averages over the last 60 days to represent the statistically steady state. This procedure is repeated systematically for various values of SST, ranging from 25° to 30°C. The resulting RCE soundings, along with the corresponding SSTs, are then used as input to the Bister and Emanuel (2002) algorithm for PI (freely available at Professor Kerry Emanuel's homepage: http://wind.mit.edu/~emanuel/home.html).

We take the SST = 27.5°C temperature profile from the RCE simulations as input for the WTG experiments. The SST is then varied in the same manner as in the RCE simulations, but as stated earlier the free-tropospheric temperature is held fixed above the boundary layer—defined here as the layer between the surface and 900 hPa. This relatively shallow layer was chosen in order to be consistent with most TC environments. [Using a boundary layer top at 850 hPa had no material effect on the results presented herein (not shown).] The moisture profile from the RCE calculation with SST = 27.5°C is also used as the reference profile toward which the WTG moisture profiles are relaxed in the representation of the horizontal advection term.

As in the RCE simulations, the mean soundings from the WTG simulations are determined by taking a time average over the last 60 days of each run. The resulting soundings are then used as inputs to the PI algorithm.

The environmental convective available potential energy (CAPE) is calculated from the Bister and Emanuel PI algorithm, as well as from a separate routine provided by G. Bryan (available from G. Bryan's Web page: http://www.mmm.ucar.edu/people/bryan/). The user options in G. Bryan's routine were chosen to be consistent with the assumptions of the environmental CAPE within the PI code [i.e., reversible adiabatic ascent, liquid only (no ice) and that the parcel is lifted from the surface].

3. Results

a. RCE and WTG climate states

Figure 1 shows the temperature profiles for the RCE and WTG runs, expressed as differences from the RCE control temperature profile (corresponding to SST = 27.5°C). In RCE, the tropospheric temperature profile is determined by a balance between convective heating and radiative cooling, and the whole temperature profile adjusts to the SST such that equilibrium is achieved between the planetary boundary layer and the moist-convective-adjusted state of the free troposphere. Thus

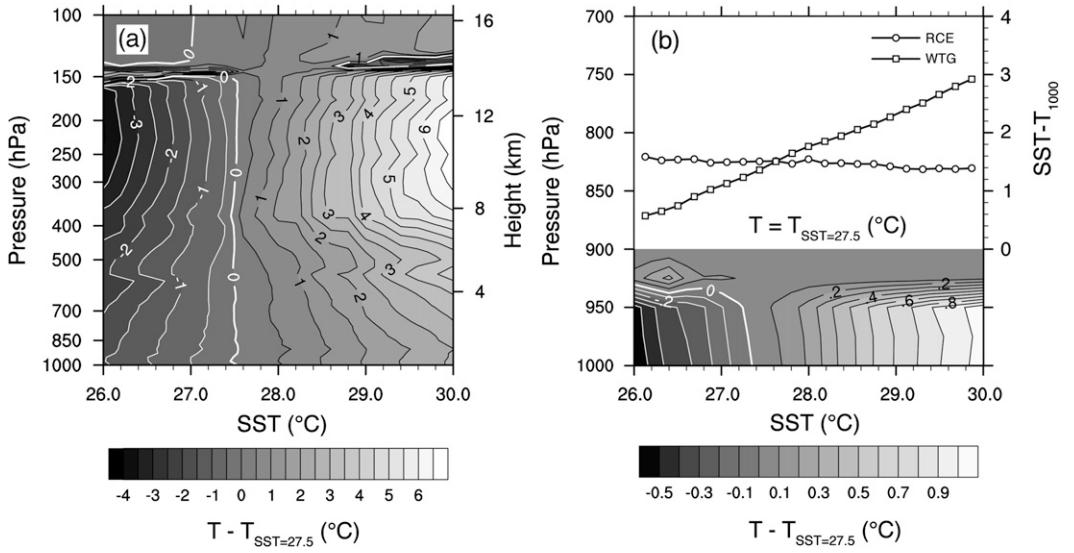

FIG. 1. (a) SST-height (pressure) contour plot of RCE temperature minus the RCE control temperature profile (SST = 27.5°C). The 0 line is shown in white. (b) As in (a), but for the WTG temperature, which only varies below 900 hPa. The lines above the contour plot show the difference between the SST and 1000-hPa temperature in RCE and WTG.

atmospheric temperature increases with SST. The boundary layer temperature increases at approximately the same rate as the SST, while the increase is larger in the upper troposphere owing to the fact that the temperature profile tends to be moist adiabatic, as in observations of variability in the tropical mean temperature profile (e.g., Santer et al. 1996; Hurrell and Trenberth 1998; Wentz and Schabel 2000; Fu et al. 2004). In the WTG simulations there is no change in the free-tropospheric temperature, by design, but the temperature within the boundary layer varies with SST, controlled by a balance between surface turbulent fluxes, radiative fluxes, and convective downdrafts (Fig. 1b). Compared to RCE, the temperature change in the WTG boundary layer is much less—by a factor of about 2.5—because the boundary layer is affected by convective downdrafts that increase with the strength of the convection. The strength of the convection, in turn, is determined by the relative buoyancy of boundary layer air, which increases much more rapidly with SST than it does in RCE, because under WTG the free-tropospheric temperature cannot increase in concert with that in the boundary layer. Similarly, there is an upward linear slope in the difference between SST and the 1000-hPa temperature in WTG, as SST is increased, whereas there is almost no trend or even a slight downward slope in RCE (Fig. 1b).

Large differences between the RCE and WTG runs can also be seen in tropospheric profiles of convective mass flux and relative humidity (Figs. 2 and 3). In RCE, the convective mass flux varies little with SST, although the height of the tropopause and thus the deep convection increases slightly (Fig. 2a). There is also little change in the profiles of relative humidity (Fig. 2b).

The WTG results reveal three distinct convective regimes depending on the SST. For sufficiently low SST, here below about 26.2°C (1.3°C less than the RCE control), the convective mass flux goes to zero at the top of the boundary layer such that there are no clouds above that level and completely dry weather prevails. In the absence of parameterized horizontal moisture advection, the free-tropospheric humidity would approach zero in this regime, as can be seen in the similar calculations without horizontal advection in Sobel and Bretherton (2000) or Sobel and Bellon (2009). For SST between 26.2° and 27°C, precipitating convection occurs but does not reach the tropopause; the cloud tops are at about 550 hPa. This regime is absent if horizontal moisture advection is neglected. Finally, for SST greater than 27°C, the convection penetrates up to, or slightly above, the tropopause. Quantitatively, the convective mass flux at 500 hPa ranges from 4.8 g m^{-2} s^{-1} for SST = 27.5°C to 29.3 g m^{-2} s^{-1} for SST = 30°C, whereas in RCE it remains relatively unchanged at about 7.6 g m^{-2} s^{-1}. Thus, in WTG the atmosphere destabilizes (stabilizes) as the SST is increased (decreased) from the RCE control value. Vertical profiles of relative humidity in WTG are shown in Fig. 3b. Above the dry limit of SST = 26.2°C, the relative humidity in the lower free troposphere increases with increasing SST. However, within the lower part of

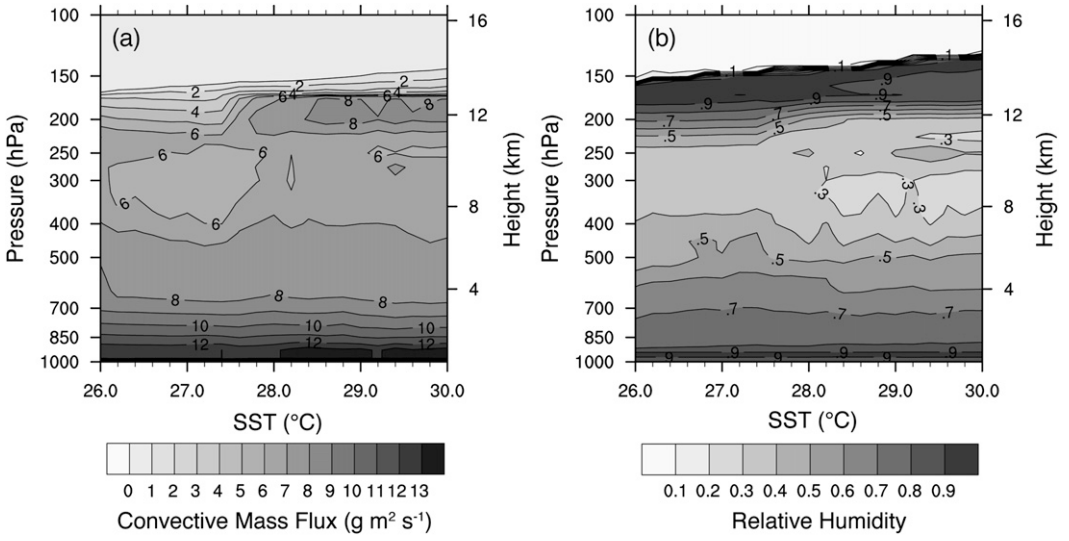

FIG. 2. SST-height (pressure) contour plots from RCE simulations of (a) convective mass (kg m^{-2} s^{-1}) and (b) relative humidity.

the boundary layer there is a slight decrease in relative humidity with increasing SST, most likely attributable to the stronger convective downdrafts associated with the stronger updrafts and greater precipitation rate, all ultimately caused by greater instability.

Finally, there are large differences in the sensitivity of precipitation rate to SST between the RCE and WTG runs (Fig. 4). In RCE, the precipitation rate is relatively steady at about 4.8 mm day^{-1}, consistent with the near-zero convective mass flux slope in Fig. 2, whereas in WTG it varies substantially from zero in the dry regime to about 28 mm day^{-1} at SST = 30°C. These slopes are consistent with the basic assumptions of RCE and WTG. In RCE, the convective heating (and precipitation) has to balance the radiative cooling, which cannot change much, whereas in WTG it can balance adiabatic cooling because of interactive vertical motion, which can vary greatly depending on surface forcing. Physically, the precipitation dependence on SST in RCE can be thought of as representing the sensitivity of global mean precipitation to SST in an aqua planet with uniform SST as that SST is varied, while the dependence under WTG can be thought of as representing that due to spatial variations in SST within a single tropical climate state.

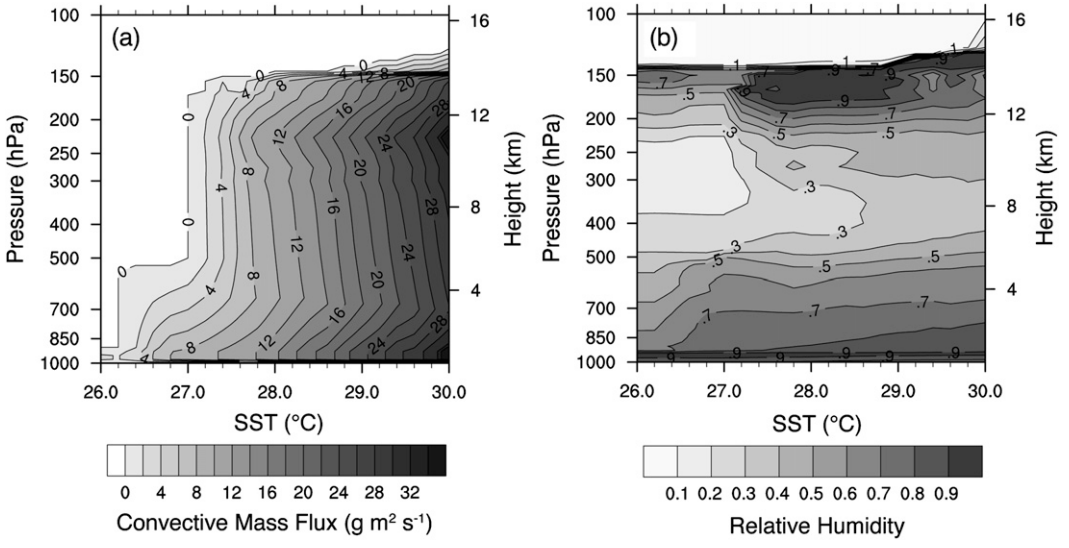

FIG. 3. As in Fig. 2, but for the WTG simulations.

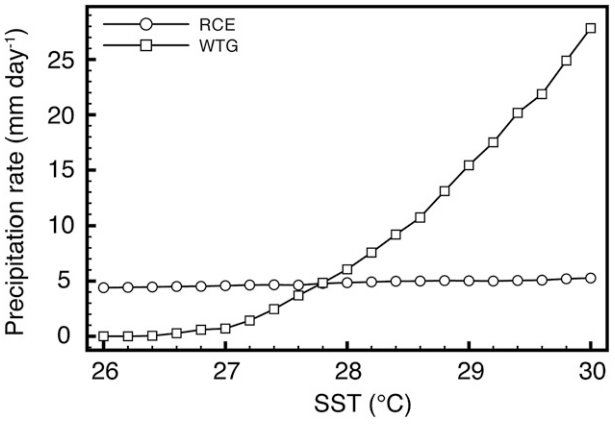

FIG. 4. Precipitation rate (mm day^{-1}) as a function of SST in RCE and WTG.

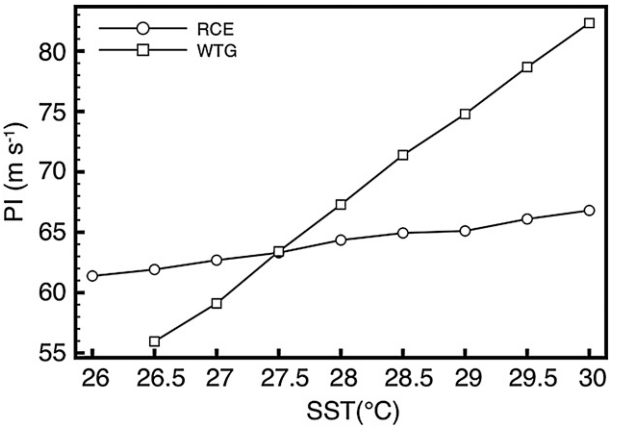

FIG. 5. The PI as a function of SST in RCE (absolute SST) and WTG (relative SST) modes.

b. Potential intensity

The sensitivities of changes in PI to changes in absolute SST (RCE simulations) and relative SST (WTG simulations) are presented in Fig. 5. For changes in absolute SST, the PI increases almost linearly from 61.4 m s^{-1} (SST = 26°C) to 66.8 m s^{-1} (SST = 30°C), or at a rate of about 1.4 m s^{-1} °C^{-1}. For changes in relative SST, the PI increases from 56.0 m s^{-1} (SST = 26.5°C) to 82.3 m s^{-1} (SST = 30°C), corresponding to a rate of 7.6 m s^{-1} °C^{-1}. This is consistent with the slope obtained from GCM and reanalysis data of about 8 m s^{-1} °C^{-1} (Vecchi and Soden 2007). Thus, PI is much more sensitive to a given change in relative SST than to the same change in absolute SST, by a factor of about 5. The slope of PI change to relative SST change is found to vary slightly, between about 7 and 8 m s^{-1} °C^{-1}, depending on the values chosen for some input parameters in the model's convection scheme, as well as whether parameterized horizontal moisture advection is included or not (see appendix).

There are two expressions commonly used to compute PI:

$$V^2 = V_R^2 \frac{T_s - T_0}{T_0} \frac{C_k}{C_D}(k^* - k), \tag{1}$$

$$V^2 = V_R^2 \frac{T_s}{T_0} \frac{C_k}{C_D}(\mathrm{CAPE}_{\mathrm{MS}} - \mathrm{CAPE}_M). \tag{2}$$

The first expression is the ''enthalpy''-based approach (e.g., Bister and Emanuel 1998), while the second is that implemented in Emanuel's code and used in this study. A key difference in (2) compared to (1) is the explicit appearance of the constant of proportionality, $(T_s - T_0)/T_s$ (the so-called thermodynamic efficiency), which is implicit in the CAPE terms. In both formulas, V is the maximum azimuthal surface wind speed (the derived quantity predicted by PI theory), T_s is the temperature at the ocean surface, C_k and C_D are the exchange coefficients for momentum and enthalpy, and V_R is a constant used to reduce the gradient wind to the 10 m wind (chosen here to be 0.8), which is not included in Bister and Emanuel (1998) but has been added here for consistency with the PI as formulated in Emanuel's PI code (2). In the first formula, T_0 is an enthalpy-weighted mean outflow temperature, and $(k^* - k)$ is the difference between the saturation enthalpy at the sea surface (k^*) and the enthalpy of the air at 10 m (k), both of which are evaluated at the radius of maximum winds (RMW). In the second formula, the outflow temperature, T_0, is calculated from a parcel lifted with temperature and relative humidity of the environment at the lowest model level, but with pressure at the RMW (thus T_0 must be computed interactively as part of the theory). The $\mathrm{CAPE}_{\mathrm{MS}}$ is the saturated CAPE at the RMW, and CAPE_M is the actual CAPE of the boundary layer air at the RMW. The ratio of C_k to C_D is assumed constant (chosen here to be 0.9), and so does not contribute to the difference in the PI slopes shown in Fig. 5. Further, the ratio of T_s to T_0 in (2) varies almost negligibly between the WTG and RCE simulations, ranging from about 1.47 to 1.48. This invariance is the result of very small changes in T_0, which in the WTG calculations ranges from 203 K at SST = 26.5°C to 205.5 K at SST = 30°C (see Fig. 6).

The two expressions for PI, Eqs. (1) and (2), are in principle equivalent, but comparing them requires a careful evaluation of the outflow temperature. Because of approximations made in the PI code, the outflow temperature that renders the two equivalent (given the other quantities in the formulas, all of which are either computed by the code or given by the input data) is not explicitly computed by the code. When using (2) to interpret results computed from the code [which, again, uses (1) for the

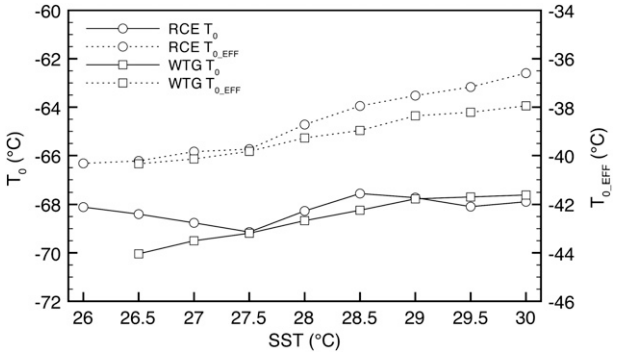

FIG. 6. The outflow temperature as used in the expression for PI from Emanuel's code (solid lines) and the effective outflow temperature (dotted lines) in RCE (circles) and WTG (squares) as a function of SST.

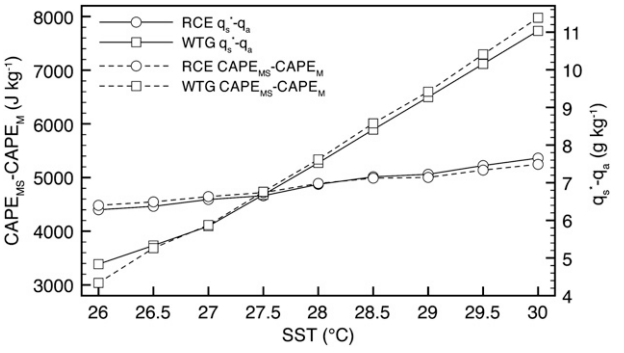

FIG. 7. The PI-relevant air–sea disequilibrium expressed as (i) the difference between saturated and unsaturated CAPE at the RMW (dashed lines) and (ii) the specific humidity change across the air–sea interface (solid lines), as a function of SST in RCE and WTG.

computation] it is best to compute T_0 a posteriori as that which makes the two equivalent. This effective T_0 (T_{0_EFF}) can be computed from the enthalpy-based PI (1) using ($k^* - k$) and the V predicted from (2). Though substantially warmer than the T_0 reported by the PI code, T_{0_EFF} is almost identical in its sensitivity to SST changes in WTG (both T_{0_EFF} and T_0 increase at a rate of about 0.74°C °C^{-1}), as shown in Fig. 6. The large discrepancy in the mean values of T_0 and T_{0_EFF} (~30°C) warrants further investigation.

The insensitivity of the outflow temperatures in (1) and (2) to SST change in the WTG calculations leaves only the thermodynamic disequilibrium ($CAPE_{MS} - CAPE_M$ or $k^* - k$) as the likely cause behind the slope differences in Fig. 5. Indeed, this turns out to be the main contributing factor to the difference in PI change between the absolute SST (RCE) and relative SST (WTG) experiments.

Figure 7 shows the sensitivity of PI-relevant (as opposed to large-scale or environmental) thermodynamic disequilibrium to SST for the two sets of experiments, expressed in terms of both ($CAPE_{MS} - CAPE_M$) and the specific humidity difference across the air–sea interface at the RMW ($q_s^* - q_a$). Like the PI slopes in Fig. 5, the air–sea disequilibrium is much more sensitive to SST change in WTG than in RCE. Taking the square root of ($CAPE_{MS} - CAPE_M$), we find that the rate of change of air–sea disequilibrium in WTG (relative SST) is about 6 times greater than in RCE (absolute SST), similar to the difference in PI slopes in Fig. 5. The disparity in the way ($CAPE_{MS} - CAPE_M$) and ($q_s^* - q_a$) respond to SST change in WTG and RCE is a consequence of the nontrivial interaction between several influences: surface fluxes, convective downdrafts, the local atmospheric thermodynamic profile, and cloud-radiative effects. Here the SST is fixed to simplify analysis, though of course in reality the amount of cloudiness and radiation would have some modifying effect. The difference in the air–sea disequilibrium slopes shown in Fig. 7 can be explained physically, at least to first order, by considering the temperature and moisture properties of the boundary layer relative to the underlying SST. For the absolute SST (RCE) experiments, the mean boundary layer (surface to 900 hPa) temperature increases at the same rate as the rate of increase of SST [i.e., 1°C (°C)$^{-1}$], as can be inferred from Fig. 1. For the relative SST (WTG) experiments, the boundary layer temperature increases much more slowly for the same increase in SST—by a factor of about a half. Because the free-tropospheric temperature is fixed, the strength of convection and particularly convective downdrafts into the boundary layer intensifies as SST increases; thereby limiting the warming and moistening of the boundary layer.

Finally, the environmental CAPE, calculated by lifting a surface-based parcel to its level of neutral buoyancy while assuming reversible adiabatic ascent, is near 0 for the absolute SST (RCE) simulations and between 0 and 100 J kg^{-1} for the relative SST (WTG) experiments (Fig. 8). Results are relatively insensitive to the choice of algorithm used to calculate CAPE (G. Bryan's method gives slightly higher CAPE in WTG than the CAPE obtained from Bister and Emanuel's PI algorithm, though their sensitivities to SST are qualitatively similar). While there are notable differences in the CAPE–SST relationship between the absolute SST and relative SST experiments (Fig. 8), these differences appear to be less directly related to the PI slopes shown in Fig. 5.

c. *Sensitivity of PI change to surface wind speed*

In this section we test the sensitivity of our results to surface wind speed, which is a free parameter in our calculations. We vary the specified mean surface wind speed from its default value of 7 m s^{-1} to a range of values from

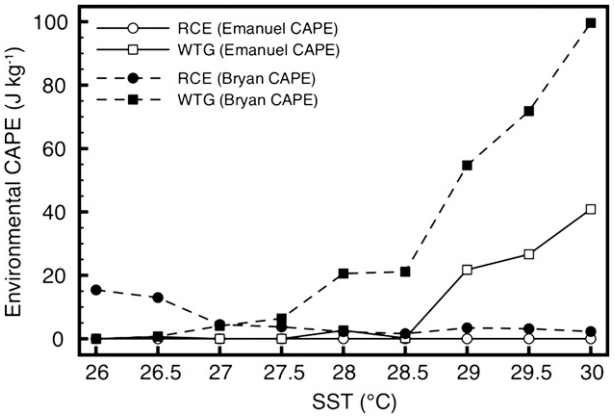

FIG. 8. As in Fig. 7, but for the environmental CAPE. Solid lines indicate CAPE calculated from K. Emanuel's PI algorithm. The dashed lines show CAPE calculated from an alternative code provided by G. Bryan. Both methods assume reversible ascent, liquid only (no ice), and that parcels are lifted from the surface.

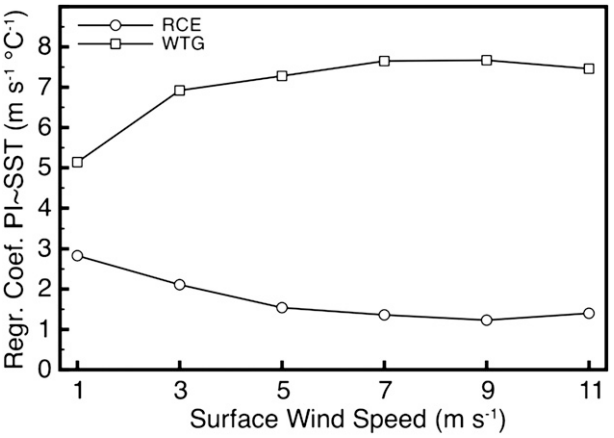

FIG. 9. Regression coefficients of the slopes of PI change to SST change in RCE and WTG as a function of mean surface wind speed.

1 to 11 m s^{-1}. Figure 9 shows the regression slopes (of PI change to SST change, as in Fig. 5) in RCE and WTG for different surface wind speeds. In RCE, the regression slopes generally increase as the wind speed decreases. The opposite is true in WTG, with a tendency for the regression slopes to decrease with decreasing wind speed. We find that for a reasonable range of wind speeds, say from 3 to 9 m s^{-1}, the sensitivity of PI change to SST change in WTG is quite small (6.9 to 7.7 m s^{-1} °C^{-1}). In RCE, the sensitivity is considerably larger (at least relatively), with regression slopes ranging from 2.1 to 1.2 m s^{-1} °C^{-1} for the same range of wind speeds.

It should be pointed out that the sensitivity of the regression slopes to the surface wind speed here where the SST is specified, will in general not be the same as the case in which the surface energy budget is closed. One would expect different dependences of PI on SST in that case if SST changes were caused by a wind speed change with the radiation and ocean heat transport fixed versus if wind speed were held constant while one of those energetic forcings were changed (see Emanuel 2007, 2010 for related discussion). In our calculations, the residual in the energy budget (see below) varies together with wind speed and is not externally constrained.

d. Surface energy budget

Since PI changes tend to be (and certainly are in our calculations) associated with changes in air–sea disequilibrium, they must also be associated in general with changes in the surface energy balance (Emanuel 2007). Although our calculations are performed at fixed SST, and thus do not satisfy an explicit energy budget, it is nonetheless relevant to analyze the changes in the terms in that budget that are computed. The residual can be interpreted as the change in those components not computed—most prominently, the tendency attributable to ocean heat transport—that would be required to sustain the simulated state.

The terms in the surface energy budget computed in the WTG simulations are shown in Fig. 10. The largest change with SST is in the latent heat flux, with smaller but still substantial changes in shortwave radiative flux, and much smaller changes in the other terms. Since the surface wind speed is held constant at 7 m s^{-1}, the latent heat flux increase is due entirely to the difference between the saturation specific humidity at the sea surface (q_s^*) and the specific humidity of air at 10 m (q_a), which to a large extent controls the air–sea thermodynamic disequilibrium in PI theory. The environmental latent heat flux and PI-relevant latent heat flux depend very similarly on SST, as can be seen by comparing Figs. 7 and 10. The environmental latent heat flux ranges from 95.8 W m^{-2} at SST = 26°C to 220 W m^{-2} at SST = 30°C. The incoming shortwave radiation shows little change up to SST = 27°C, after which it decreases steadily owing to increased cloudiness, particularly in the upper troposphere (Fig. 3b). The shortwave flux varies from 294.9 to 225.2 W m^{-2} over the range of SST shown. This value is likely to be model dependent, depending on the cloud and radiative parameterizations as well as on our choice of insolation (400 W m^{-2} with no diurnal cycle).

The residual in the surface energy budget varies by 217.7 W m^{-2} over the entire range of SST shown or a rate of roughly 54 W m^{-2} °C^{-1}. This is a very strong sensitivity; to the extent that it represents reality, it indicates that relative SST cannot change dramatically without a radical reorganization of the tropical ocean circulation. On the other hand, the tropical oceans currently support

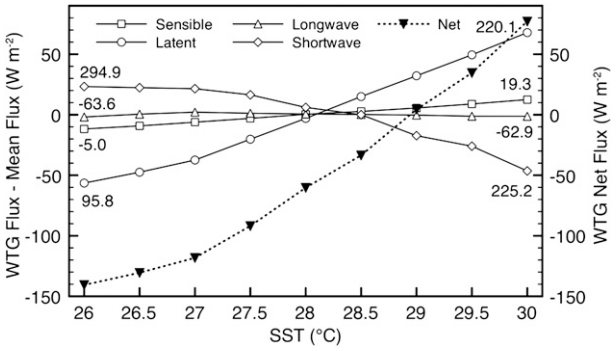

FIG. 10. Components of the WTG surface energy budget as a function of SST. The mean flux of each component has been subtracted from the actual values to make comparison easier. The actual flux values are plotted next to the points corresponding to SST = 27.5°C and SST = 30°C. The net flux (sensible + latent − longwave − shortwave) is indicated by the bold dotted curve.

spatial SST variations of several degrees, so changes in relative SST of a degree or two do not seem inconceivable. In any case, since the dependence of PI on relative SST in our calculations is quite linear over most of the range shown here, our calculations can simply be interpreted as estimates of that dependence that are valid for either small changes in relative SST or large ones, should the latter somehow occur.

4. Relationship with observations and more comprehensive models

Vecchi and Soden (2007) used reanalyses and climate model projections to analyze the relationship between PI and both relative and absolute SST. They defined a proxy index for PI change as the difference between the tropical mean SST change and the local SST change: $\mathrm{PI}(x, y, t) \equiv [\Delta\mathrm{SST}(x, y, t) - \langle\Delta\mathrm{SST}(t)\rangle)$, and the tropical mean SST ($\langle\mathrm{SST}(t)\rangle$) as the area average SST over the domain 30°S–30°N. They computed statistics based on a linear least squares fit for the period 1958–2002 using two reanalysis products—40-yr European Centre for Medium-Range Weather Forecasts (ECMWF) Re-Analysis (ERA-40) and National Centers for Environmental Prediction (NCEP). SST and PI are averaged over the months June–November. Based on this simple linear model, they find that PI increases by about 8–8.5 m s^{-1} per degree of relative SST increase. The change in tropical mean PI per tropical mean SST change was found to be an order of magnitude smaller and opposite in sign (-0.63 m s^{-1} °C^{-1} for ERA-40 and -1.17 m s^{-1} °C^{-1} for NCEP). They also found considerable uncertainty in the slope of tropical mean PI based on the Intergovernmental Panel on Climate Change Fourth Assessment Report (IPCC AR4) models using scenario A1B (balanced emphasis on all energy sources), with some models giving a negative slope and others giving a positive slope; the mean and median slope being slightly positive (0.27 and 0.50 m s^{-1} °C^{-1}).

Results from the RCE simulations presented here suggest that the tropical mean PI should increase slightly in response to uniform SST warming (1.4 m s^{-1} °C^{-1}). Interestingly, this result is close to those of Nolan et al. (2007) in idealized simulations with a cloud-resolving model; depending on the Coriolis parameter, they found PI increases of 1.4–2.0 m s^{-1} °C. It is also broadly consistent with the ensemble-mean IPCC AR4 results, to the extent that it is positive and much smaller than the dependence of PI on relative SST, but differs in sign from the 1958–2002 global reanalysis regression slope. The long-term reanalysis regression slopes may be partly influenced by data inhomogeneity issues in NCEP and ERA-40. It may also be to some extent inappropriate to compare our RCE results to variations in tropical mean PI. The earth is not an aqua planet with uniform SST, and spatial structure in the SST field (as well as the presence of land) may have nontrivial effects on the mean PI field that cannot be captured in single-column calculations forced by a single value of SST.

The picture is much clearer and more consistent with regard to the relationship between relative SST and PI. Vecchi and Soden (2007) found good agreement between the reanalysis data and the AR4 A1B future climate model projections, with both indicating an increase of about 8 m s^{-1} °C^{-1}. The relationship between PI and relative SST found in our WTG calculations of 7.6 m s^{-1} °C^{-1} is therefore in good agreement with GCM and reanalysis regression slopes.

A preliminary analysis of the factors contributing to the PI change in the AR4 A1B projections shows, however, that while dependence of PI on relative SST is similar to that in our calculations, the details are different, in that the outflow temperature changes are larger in the GCMs while the air–sea disequilibrium changes are smaller; that is, the GCMs would show larger slopes in a plot like Fig. 6 and smaller slopes in a plot like Fig. 7 (G. Vecchi 2010, personal communication). It appears that the convective downdraft feedback on the boundary layer is too strong in our WTG calculations compared to the GCMs, but that the outflow temperature varies less to compensate so that the resulting PI is the same. Whether this apparent compensation is accidental or related to some more fundamental control on PI is the subject of ongoing investigation.

5. Conclusions

Using a single-column model in RCE and WTG modes to represent the response of the tropical atmospheric

sounding to absolute and relative SST changes, we have shown that PI is much more sensitive to changes in relative SST than to changes in absolute SST, in agreement with several observational and GCM-based studies (Vecchi and Soden 2007; Swanson 2008; Vecchi et al. 2008). The slope of PI change to relative SST change in WTG, of 7.6 m s^{-1} °C^{-1}, is comparable in magnitude to the GCM ensemble-mean slope of 8.22 m s^{-1} °C^{-1} reported by Vecchi and Soden (2007). The slope of PI change to absolute SST change from the RCE simulations is 1.4 m s^{-1} °C^{-1}.

The greater sensitivity of PI to SST in WTG (relative SST), relative to RCE (absolute SST), can be attributed to a greater rate of increase in the air–sea thermodynamic disequilibrium with increasing SST. The greater sensitivity of air–sea disequilibrium to SST change in WTG is the result of stronger (weaker) convective downdrafts, which act to cool (warm) the boundary layer. Changes in SST have much less effect on the strength of convection in RCE, where those changes represent absolute SST changes, than they do in WTG where they represent relative SST changes. Consequently, the change in air–sea disequilibrium for a given SST change is smaller in RCE than in WTG, reducing the slope of PI (1.4 m s^{-1} °C^{-1}).

Large SST changes in our WTG calculations are accompanied by large changes in the net thermal energy flux from the ocean to the atmosphere, of the order of 50 W m^{-2} °C^{-1}. This suggests that the magnitude of relative SST changes is likely to be limited as the climate changes, since this surface flux must be balanced by changes in ocean heat transport. Nonetheless, the much greater sensitivity of PI to relative SST than absolute SST suggests that for small climate changes, changes to the spatial structure of the SST field are likely to dominate the changes to the PI field even if they are also relatively small. Under sufficiently large climate changes, however, it is reasonable to suppose that changes in the mean SST will eventually become much larger than those in the spatial SST variations, to the point that the absolute SST change may eventually be the dominant contributor to the PI change. To be able to make such statements with greater confidence, we need to reduce the uncertainty in our estimates of the expected relationship of PI to mean SST under plausible climate changes.

Acknowledgments. This work was influenced by stimulating discussions with Suzana Camargo, Kerry Emanuel, Tom Knutson, and Gabe Vecchi; we thank Kerry Emanuel and Gabe Vecchi for constructive comments on an earlier draft. HAR acknowledges support by an appointment to the NASA Postdoctoral Program at the Goddard Institute for Space Studies, administered by Oak Ridge Associated Universities through a contract with NASA. AHS acknowledges support from NOAA Grant NA08OAR4320912. The statements, findings, conclusions, and recommendations do not necessarily reflect the views of NASA, NOAA, or the Department of Commerce.

APPENDIX

Parameter Changes in the Model's Convection Scheme

The parameters modified from the default values in the convection scheme are TL_{CRIT}, the critical temperature below which the autoconversion threshold is assumed to be 0°C; σ_D, the fractional area covered by the unsaturated downdraft; and α, the rate at which the convective mass flux is relaxed toward its equilibrium value. The default values for these parameters are $TL_{CRIT} = -55$°C, $\sigma_D = 0.05$, and $\alpha = 0.02$. The modified values are $TL_{CRIT} = -50$°C, $\sigma_D = 0.1$, and $\alpha = 0.01$. Exclusion of parameterized moisture advection reduced the PI slope to 6.9 m s^{-1} °C^{-1}.

REFERENCES

Bister, M., and K. A. Emanuel, 1998: Dissipative heating and hurricane intensity. *Meteor. Atmos. Phys.,* **52,** 233–240.

——, and ——, 2002: Low frequency variability of tropical cyclone potential intensity, 1. Interannual to interdecadal variability. *J. Geophys. Res.,* **107,** 4801, doi:10.1029/2001JD000776.

Bony, S., and K. A. Emanuel, 2001: A parameterization of the cloudiness associated with cumulus convection; evaluation using TOGA COARE data. *J. Atmos. Sci.,* **58,** 3158–3183.

Bryan, G. H., and R. Rotunno, 2009: Evaluation of an analytical model for the maximum intensity of tropical cyclones. *J. Atmos. Sci.,* **66,** 3042–3060.

Emanuel, K. A., 1986: An air–sea interaction theory for tropical cyclones. Part I: Steady-state maintenance. *J. Atmos. Sci.,* **43,** 585–605.

——, 1991: A scheme for representing cumulus convection in large-scale models. *J. Atmos. Sci.,* **48,** 2313–2329.

——, 2005: Increasing destructiveness of tropical cyclones over the past 30 years. *Nature,* **436,** 686–688.

——, 2007: Environmental factors affecting tropical cyclone power dissipation. *J. Climate,* **20,** 5497–5509.

——, 2010: Tropical cyclone activity downscaled from NOAA-CIRES reanalysis, 1908–1958. *J. Adv. Model. Earth Syt.,* **2,** 1–12.

——, and M. Živković-Rothman, 1999: Development and evaluation of a convection scheme for use in climate models. *J. Atmos. Sci.,* **56,** 1766–1782.

Fouquart, Y., and B. Bonnel, 1980: Computation of solar heating of the earth's atmosphere: A new parameterization. *Beitr. Phys. Atmos.,* **53,** 35–62.

Fu, Q., C. M. Johanson, S. G. Warren, and D. J. Seidel, 2004: Contribution of stratospheric cooling to satellite-inferred tropospheric temperature trends. *Nature,* **429,** 55–58.

Held, I. M., 2005: The gap between simulation and understanding in climate modeling. *Bull. Amer. Meteor. Soc.,* **86,** 1609–1614.

Holland, G. J., 1997: The maximum potential intensity of tropical cyclones. *J. Atmos. Sci.,* **54,** 2519–2541.

Hoyos, C. D., P. A. Agudelo, P. J. Webster, and J. A. Curry, 2006: Deconvolution of the factors contributing to the increase in global hurricane intensity. *Science,* **312,** 94–97.

Hurrell, J. W., and K. E. Trenberth, 1998: Difficulties in obtaining reliable temperature trends: Reconciling the surface and satellite microwave sounding unit records. *J. Climate,* **11,** 945–967.

Kossin, J. P., K. R. Knapp, D. J. Vimont, R. J. Murnane, and B. A. Harper, 2007: A globally consistent reanalysis of hurricane variability and trends. *Geophys. Res. Lett.,* **34,** L04815, doi:10.1029/2006GL028836.

Kruk, M. C., K. R. Knapp, and D. H. Levinson, 2010: A technique for combining global tropical cyclone best track data. *J. Atmos. Oceanic Technol.,* **27,** 680–692.

Landsea, C. W., B. A. Harper, K. Hoarau, and J. A. Knaff, 2006: Can we detect trends in extreme tropical cyclones? *Science,* **313,** 452–454.

Montgomery, M. T., V. S. Nguyen, J. Persing, and R. K. Smith, 2009: Do tropical cyclones intensify by WISHE? *Quart. J. Roy. Meteor. Soc.,* **135,** 1697–1714.

Morcrette, J.-J., 1991: Radiation and cloud radiative properties in the European Centre for Medium Range Weather Forecasts forecasting system. *J. Geophys. Res.,* **96,** 9121–9132.

Nolan, D. S., E. D. Rappin, and K. A. Emanuel, 2007: Tropical cyclogenesis sensitivity to environmental parameters in radiative–convective equilibrium. *Quart. J. Roy. Meteor. Soc.,* **133,** 2085–2107.

Pasquero, C., and K. Emanuel, 2008: Tropical cyclones and transient upper-ocean warming. *J. Climate,* **21,** 149–162.

Raymond, D. J., and X. Zeng, 2005: Modelling tropical atmospheric convection in the context of the weak temperature gradient approximation. *Quart. J. Roy. Meteor. Soc.,* **131,** 1301–1320.

Rennó, N. O., K. A. Emanuel, and P. H. Stone, 1994a: Radiative–convective model with an explicit hydrologic cycle. 1: Formulation and sensitivity to model parameters. *J. Geophys. Res.,* **99,** 14 429–14 441.

——, P. H. Stone, and K. A. Emanuel, 1994b: Radiative–convective model with an explicit hydrologic cycle. 2: Sensitivity to large changes in solar forcing. *J. Geophys. Res.,* **99,** 17 001–17 020.

Santer, B. D., and Coauthors, 1996: A search for human influences on the thermal structure of the atmosphere. *Nature,* **382,** 39–46.

Schade, L. R., 2000: Tropical cyclone intensity and sea surface temperature. *J. Atmos. Sci.,* **57,** 3122–3130.

Sessions, S. L., S. Sugaya, D. J. Raymond, and A. H. Sobel, 2010: Multiple equilibria in a cloud resolving model. *J. Geophys. Res.,* **115,** D12110, doi:10.1029/2009JD013376.

Smith, R. K., M. T. Montgomery, and S. Vogl, 2008: A critique of Emanuel's hurricane model and potential intensity theory. *Quart. J. Roy. Meteor. Soc.,* **134,** 551–561.

Sobel, A. H., and C. S. Bretherton, 2000: Modeling tropical precipitation in a single column. *J. Climate,* **13,** 4378–4392.

——, and G. Bellon, 2009: The effect of imposed drying on parameterized deep convection. *J. Atmos. Sci.,* **66,** 2085–2096.

——, I. M. Held, and C. S. Bretherton, 2002: The ENSO signal in tropical tropospheric temperature. *J. Climate,* **15,** 2702–2706.

——, G. Bellon, and J. Bacmeister, 2007: Multiple equilibria in a single-column model of the tropical atmosphere. *Geophys. Res. Lett.,* **34,** L22804, doi:10.1029/2007GL031320.

Swanson, K. L., 2008: Nonlocality of Atlantic tropical cyclone intensities. *Geochem. Geophys. Geosyst.,* **9,** Q04V01, doi:10.1029/2007GC001844.

Vecchi, G. A., and B. J. Soden, 2007: Effect of remote sea surface temperature change on tropical cyclone potential intensity. *Nature,* **450,** 1066–1070.

——, K. L. Swanson, and B. J. Soden, 2008: Whither hurricane activity? *Science,* **322,** 687–689, doi:10.1126/science.1164396.

Webster, P. J., G. J. Holland, J. A. Curry, and H.-R. Chang, 2005: Changes in tropical cyclone number, duration and intensity in a warming environment. *Science,* **309,** 1844–1846.

Wentz, F. J., and M. Schabel, 2000: Precise climate monitoring using complementary satellite data sets. *Nature,* **403,** 414–416.

Wing, A. A., A. H. Sobel, and S. J. Camargo, 2007: Relationship between the potential and actual intensities of tropical cyclones on interannual time scales. *Geophys. Res. Lett.,* **34,** L08810, doi:10.1029/2006GL028581.